Self-Assembly Structures of Nonionic Surfactants at Graphite/Solution Interfaces

Heather N. Patrick,[†,‡] Gregory G. Warr,*[,†,§] Srinivas Manne,[‡,||] and Ilhan A. Aksay[‡]

School of Chemistry, University of Sydney, NSW 2006, Australia, Princeton Materials Institute and Department of Chemical Engineering, Princeton University, Princeton, New Jersey 08544, and Rhone-Poulenc/CNRS Complex Fluids Laboratory, Cranbury, New Jersey 08512

Received March 6, 1997. In Final Form: May 13, 1997[⊗]

The interfacial self-assembly structures of a series of poly(oxyethylene) *n*-dodecyl ether ($C_{12}E_n$) nonionic surfactants on graphite has been imaged by atomic force microscopy using only the steric stabilization force as the contrast mechanism. Aggregates are arranged in parallel stripes perpendicular to the underlying graphite symmetry axes for $C_{12}E_5$−$C_{12}E_{10}$. These are interpreted as hemicylindrical micelles, consistent with previous studies of ionic surfactants adsorbed on graphite. $C_{12}E_{23}$ shows a featureless layer and $C_{12}E_3$ forms an anchored lamellar phase growing normal to the graphite surface. We relate the interfacial structures to those formed in bulk solution and show that the initially adsorbed molecules template the interfacial aggregates, modifying their self-assembly behavior.

Introduction

The self-assembly of amphiphilic molecules in bulk solution is often described using the surfactant packing parameter, v/a_0l_c.[1] This quantity conveniently captures the key features of the molecular geometry: alkyl chain volume, v; alkyl chain length, l_c; interfacial area, a_0, of a surfactant molecule into a dimensionless ratio describing the interfacial curvature of a self-assembly phase. A connection between the surfactant packing parameter and the mean and Gaussian curvatures of such interfaces has recently been established.[2] Among the triumphs of the surfactant packing parameter has been its successful application to explain the phase behavior of poly(ethylene oxide) nonionic surfactants.[3] The observed sequence of phases accompanying changes in alkyl or ethoxy chain structure is easily rationalized in terms of changes to the surfactant geometry.

Recent studies of amphiphilic self-assembly structures formed by ionic surfactants at solid/solution interfaces using the atomic force microscope (AFM) have revealed that many of the aggregate geometries seen in bulk solution also occur near an interface. A number of cationic surfactants have been studied on graphite,[4] on mica,[5] and on gold[6] revealing spherical, cylindrical, and planar geometries. An anionic surfactant, sodium dodecyl sulfate, was studied on graphite.[7] A zwitterionic surfactant has also been studied on graphite, mica and silicon nitride.[8] These studies all use double-layer (noncontact) forces to image the adsorbed structure nondestructively.[9]

Nonionic surfactant adsorption on a number of solid surfaces has been studied by a variety of techniques. The forces between mica surfaces in solutions of pentakis-(oxyethylene) dodecyl ether with added electrolyte were studied by Rutland and Christenson using the surface force apparatus.[10] They found that adsorption was weak. Force measurements on silica surfaces in solutions of the same nonionic surfactant, also with added salt, showed repulsive steric forces, indicating the presence of adsorbed surfactant.[11] With the exception of mica, adsorption isotherms usually show strong, cooperative adsorption below the critical micelle concentration (cmc)[12,13] from which the existence of aggregates has been inferred.[14,15] Fluorescent probes,[16−18] ellipsometry,[19] and neutron reflectivity[20−22] all provide more direct evidence for the existence of molecular aggregates on solid substrates, although their geometries remain unknown.

Nonionic surfactants have previously been found to adsorb strongly to graphite.[12,13] Adsorption increases with increasing concentration up to the cmc, after which it remains fairly constant. We describe here an AFM study of a series of nonionic surfactants adsorbed onto graphite using *soft contact* imaging. We have found that nonionic surfactants on graphite give force profiles exhibiting short-range repulsion that can be used for imaging in a manner similar to electrostatic imaging. The existence of such steric stabilization forces induced by adsorbed layers in

* E-mail: g.warr@chem.usyd.edu.au.
† University of Sydney.
‡ Princeton University.
§ Rhone-Poulenc/CNRS Complex Fluids Laboratory.
|| Current address: Department of Physics, University of Arizona, Tucson, AZ 85721.

⊗ Abstract published in *Advance ACS Abstracts,* July 1, 1997.

(1) Israelachvili, J. N.; Mitchell, D. J.; Ninham, B. W. *J. Chem. Soc., Faraday Trans. 2* **1976**, *72*, 1525−1568.
(2) Hyde, S. T. *Colloids Surf., A* **1995**, *103*, 227.
(3) Mitchell, D. J.; Tiddy, G. J. T.; Waring, L.; Bostock, T.; McDonald, M. P. *J. Chem. Soc., Faraday Trans. 1* **1983**, *79*, 975−1000.
(4) Manne, S.; Cleveland, J. P.; Gaub, H. E.; Stucky, G. D.; Hansma, P. K. *Langmuir* **1994**, *10*, 4409−4413.
(5) Manne, S.; Gaub, H. E. *Science* **1995**, *270*, 1480−1482.
(6) Jaschke, M.; Butt, H.-J.; Gaub, H. E.; Manne, S. *Langmuir* **1997**, *13*, 1381−1384.
(7) Wanless, E. J.; Ducker, W. A. *J. Phys. Chem.* **1996**, *100*, 3207−3214.
(8) Ducker, W. A.; Grant, L. M. *J. Phys. Chem.* **1996**, *100*, 11507−11511.
(9) Senden, T. J.; Drummond, C. J.; Kékicheff, P. *Langmuir* **1994**, *10*, 358−362.
(10) Rutland, M. W.; Christenson, H. K. *Langmuir* **1990**, *6*, 1083−1087.
(11) Rutland, M. W.; Senden, T. J. *Langmuir* **1993**, *9*, 412−418.
(12) Aston, J. R.; Furlong, D. N.; Grieser, F.; Scales, P. J.; Warr, G. G. In *Adsorption at the Gas/Solid and Liquid-Solid Interface*; Rouquerol, J., Sing, K. S. W., Eds.; Elsevier: New York, 1982; pp 97−102.
(13) Findenegg, G. H.; Pasucha, B.; Strunk, H. *Colloids Surf.* **1989**, *37*, 223−233.
(14) Portet, F.; Desbene, P. L.; Treiner, C. *J. Colloid Interface Sci.* **1996**, *184*, 216.
(15) Böhmer, M. R.; Koopal, L. K. *Langmuir* **1990**, *6*, 1478.
(16) Levitz, P.; El Meri, A.; Keravis, D.; Van Damme, H. *J. Colloid Interface Sci.* **1984**, *99*, 484.
(17) Levitz, P.; Van Damme, H.; Keravis, D. *J. Phys. Chem.* **1984**, *88*, 2228−2235.
(18) Levitz, P.; Van Damme, H. *J. Phys. Chem.* **1986**, *90*, 1302.
(19) Tiberg, F.; Jonsson, B.; Tang, J.; Lindman, B. *Langmuir* **1994**, *10*, 2294.
(20) Lee, E. M.; Thomas, R. K.; Cummins, P. G.; Staples, E. J.; Penfold, J.; Rennie, A. R. *Chem. Phys. Lett.* **1989**, *162*, 196.
(21) McDermott, D. C.; Lu, J. R.; Lee, E. M.; Thomas, R. K.; Rennie, A. R. *Langmuir* **1992**, *8*, 1204.
(22) Böhmer, M. R.; Koopal, L. K.; Janssen, R.; Lee, E. L.; Thomas, R. K.; Rennie, A. R. *Langmuir* **1992**, *8*, 2228.

S0743-7463(97)00254-0 CCC: $14.00

colloidal dispersions has long been known.[23] Their role in the interaction between surfaces, for both adsorbed polymers[24] and adsorbed nonionic surfactants,[25] has been studied using the surface force apparatus. This is the first time the technique of imaging surfactant aggregates has been used in truly uncharged surfactant solutions with no possibility of double layer forces being present.

We seek here to determine the relationship between bulk solution aggregation patterns and those observed at a solid interface for a series of nonionic poly(ethylene oxide) dodecyl ethers in which the surfactant packing parameter is systematically varied. The effect of changes in the degree of ethoxylation and hence v/a_0l_c on self-assembly structures formed on graphite is studied using atomic force microscopy imaging.

Experimental Procedure

Surfactants. The surfactants under study were the poly(ethylene oxide) alkyl ethers: tris(ethylene oxide) dodecyl ether ($C_{12}E_3$), $C_{12}E_5$, $C_{12}E_8$, $C_{12}E_9$ (all Fluka), $C_{12}E_{10}$ (Sigma), and $C_{12}E_{23}$ (Brij 35, Fluka). $C_{12}E_{10}$ was found to be polydisperse by MALDI-TOF and contained a distribution of head group chain lengths with a standard deviation of 3 ethylene oxide units. Brij 35 was also polydisperse. All other surfactants were >96% monodisperse.

Polarizing Microscopy. Polarizing microscopy was used to identify the sequence of phases for a surfactant. A flooding experiment was performed where a drop or small crystal of the surfactant was placed next to a drop of water on a slide before a cover slip was placed over them both. The resulting concentration gradient produces the full sequence of phases present in a surfactant/water mixture. Observation through crossed polarizing lenses showed isotropic phases as dark and liquid crystals as distinctive patterns. Cubic (viscous isotropic) phases next to isotropic (micellar) phases could be identified at their boundaries due to the refractive index change. Bubbles trapped at this interface also show characteristic deformations due to the yield stress of the cubic phase.

AFM Imaging. The substrate used was a graphite monochromator grade ZYH from Advanced Ceramics, OH. This was freshly cleaved for each experiment using adhesive tape. The AFM used was a Digital Instruments (DI) Nanoscope III used in contact mode. Surfactant aggregates were imaged in deflection mode with low feedback gains. (Typical values are integral gain 0.3, all others 0.) Scan rates were between 5 and 14 Hz. No filtering of the images was performed other than flattening along the scan lines. The tips were standard silicon nitride cantilevers (DI) irradiated for 30−40 min by UV light prior to their use. They had nominal spring constants of 0.3 N m^{-1}. All measurements were performed at room temperature using a liquid cell. Solutions were equilibrated for 0.5−4 h before the start of the experiment to minimize thermal drift.

The imaging technique used here is similar to that described previously.[4,5,26] Briefly, the tip is brought toward the surface to where it experiences a repulsive force, but before it pushes through the adsorbed layer. The force on the tip is set near to, but below, this breakthrough force. This set point is maintained throughout an AFM image scan. In previous experiments the repulsive force was a noncontact effect attributed to electrical double-layer interactions. The repulsion experienced by the cantilever in these experiments however is purely a steric one, due to contact between the coated substrate and the AFM tip (which may also be coated with surfactant). Imaging by this *soft contact* method is very delicate, and tip breakthrough often occurs, revealing the underlying graphite lattice. Nevertheless, reproducible scans were reliably obtained for all surfactants if low forces were employed.

(23) Napper, D. H. *Polymeric Stabilization of Collidal Dispersions*; Academic Press: London, 1983.
(24) Israelachvili, J. N. *Intermolecular and Surface Forces*, 2nd ed.; Academic Press: London, 1992.
(25) Claesson, P. M.; Kjellander, R.; Stenius, P.; Christenson, H. K. *J. Chem. Soc., Faraday Trans. 1* **1986**, *82*, 2735−2746.
(26) Manne, S. *Prog. Colloid Polym. Sci.*, in press.

Table 1. Summary of Phase Sequences for Poly(ethylene oxide) Dodecyl Ethers in Water at Room Temperature (~25 °C)

surfactant	cloud point (°C)	cmc (mM)	phase sequence with increasing surfactant concentration[b]
$C_{12}E_3$[a]	<0		W L_α L_2
$C_{12}E_5$[a]	26.5	0.064[27]	L_1 *c* *c* L_α L_2
$C_{12}E_8$[a]	77	0.081[29,29]	L_1 H_1 V_1 *c* L_2
$C_{12}E_9$		0.1[30]	L_1 I_1 H_1 L_2
$C_{12}E_{10}$			L_1 H_1 L_2
$C_{12}E_{23}$		0.1[30]	L_1 I_1 L_2

[a] From ref 3. [b] We define the phases as follows: W, water containing surfactant monomer; L_1, micellar solution; I_1, cubic phase of close packed spherical micelles; H_1, hexagonally packed rodlike micelles; V_1, bicontinuous cubic phase; L_α, lamellar phase; L_2, "surfactant liquid". [c] $C_{12}E_5$: H_1 phase melts 18.5 °C; V_1 phase melts 20 °C. $C_{12}E_8$: L_α phase melts 22 °C.

Results

1. Bulk Self-Assembly Behavior. The room temperature, bulk phase behavior of the surfactants studied is listed in Table 1. The full sequence of phases from low to high surfactant concentration is shown in Figure 1 for (a) $C_{12}E_9$, (b) $C_{12}E_{10}$ (polydisperse), and (c) $C_{12}E_{23}$ (Brij 35, polydisperse).

$C_{12}E_9$ forms, at low concentration, an isotropic phase (L_1) followed by a cubic (isotropic) phase (I_1). A hexagonal phase (H_1) follows, then a third isotropic phase (L_2), and finally solid surfactant. $C_{12}E_{10}$ forms an isotropic solution phase (L_1) followed by a hexagonal phase (H_1) and then an isotropic phase (L_2) and solid surfactant crystals. Brij 35 forms a solution phase (L_1) followed by a cubic phase (I_1). The boundary between these two phases can be seen by the eye and is also indicated by the air bubbles crossing the interface. Within the cubic phase, the bubbles are deformed due to the yield stress of the material, whereas in a liquid isotropic phase they are spherical. At higher concentrations an L_2 phase and crystalline phases are observed.

The phase structures depend on the number of ethylene oxide units in the head group, which is related to the surfactant packing parameter v/a_0l_c.[1] For the series studied in this work, the alkyl tail was kept constant at 12 carbons and the number of ethylene oxide units was varied between 3 and 23.

Table 1 summarizes surfactant geometry as a function of two parameters, ethylene oxide number and concentration. Alkyl chain length and volume are constant in this series, and interfacial area, a_0, is determined by the (steric) interactions between ethylene oxide chains within an aggregate. Increasing ethylene oxide number thus increases a_0 by increasing the radius of gyration of the chain. On the other hand, increasing concentration decreases a_0 due to the lower water activity and hence reduced hydration of each chain.

Increasing the head group size while keeping the hydrophobic portion of the molecule constant decreases v/a_0l_c. This corresponds to an increase in the interfacial curvature of the aggregate. Small a_0 leads to planar interface and hence a lamellar phase. Larger a_0 causes cylindrical aggregates to form, leading to a hexagonal phase. Even larger a_0 will allow only spheres, and this leads to a close-packed micellar cubic phase (I_1). For the series studied, this is seen firstly in the structure of the most dilute liquid crystalline phase. The first mesophase formed after the micellar solution varies from lamellar for $C_{12}E_3$ and $C_{12}E_5$ to hexagonal for $C_{12}E_8$ to I_1 cubic for $C_{12}E_9$. The polydisperse Brij 35 contains an average head group size of 23 and only forms a cubic spherical micellar

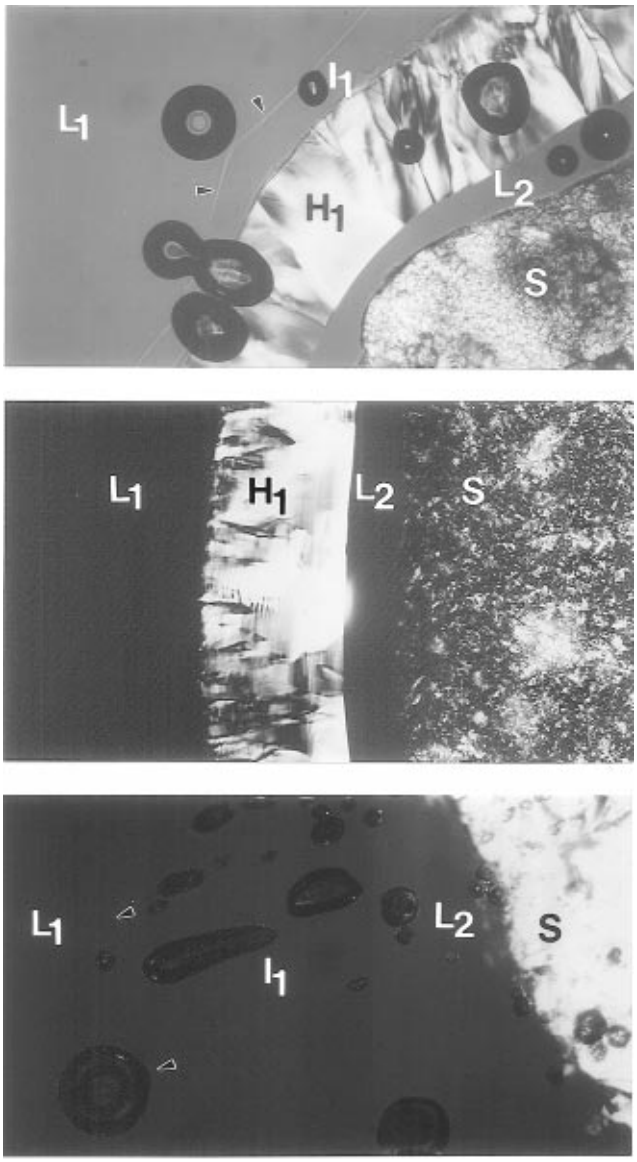

Figure 1. Photographs of polarizing microscopy flooding experiments of (a, top) $C_{12}E_9$, (b, middle) $C_{12}E_{10}$, and (c, bottom) $C_{12}E_{23}$ (Brij 35). Concentration increases from left to right. Phases are labeled as follows: isotropic (micellar) L_1, isotropic (cubic) I_1, hexagonal H_1, isotropic L_2, solid surfactant, S. The L_1/I_1 phase boundary is indicated by deformed bubbles and by a refractive index change shown by arrows in (a) and (c).

phase, as observed by polarizing microscopy, Figure 1c. As has been noted previously, the polydisperse $C_{12}E_{10}$ is out of sequence and behaves as though it contains fewer ethoxy groups.[3]

Similarly, as concentration is increased, a_0 decreases and interfacial curvature follows the reverse sequence from spheres toward planes for each of these surfactants.[3]

2. Interfacial Self-Assembly Behavior. The self-assembly structures formed by adsorbed surfactant were studied on a freshly cleaved graphite surface. All surfactants were studied in solutions greater than twice their cmc,[27−30] which is sufficient to ensure surface saturation.

Force profiles were obtained for each solution after their injection into the AFM liquid cell. Figure 2 shows the force profiles for $C_{12}E_n$ solutions on graphite ($n = 5$, 8, 9, 10, and 23). Although quantitative force information is difficult to obtain due to the uncertain geometry of the AFM tip, certain general conclusions can be drawn. The surfactants all display similar force curves as a function of tip−surface separation. On approach, the force on the cantilever increases from zero to a point where there is a breakthrough through an adsorbed layer between the tip and the surface. At this point the tip is in contact with the surface which can be imaged at this force. This is the usual method of imaging a solid surface known as contact mode. Surfactant layers are imaged in soft contact mode by using applied forces lower than that necessary to break through to the substrate. In the absence of surfactant, approach of the tip to the surface produces an adhesive jump into contact with no repulsive wall. This is strong evidence for the presence of an adsorbed film of surfactant, which is certainly expected at concentrations above the cmc.[12,13]

It is apparent from Figure 2 that the range of the repulsive steric stabilization force increases with the ethylene oxide number. This is consistent with the increased length of the hydrophilic head groups of these amphiphiles. The force profile is well described by an exponential function of distance, as is seen for adsorbed polymers in the surface force apparatus,[24] whose range should scale with the radius of gyration of the hydrophilic ethoxy groups. A log−log fit of decay length versus ethoxy number yields an exponent of 0.61 ± 0.11, which is close to the expected 0.5 for a random coil. Figure 3 shows the decay lengths of the force curves against square root of ethoxy number. Despite some experimental scatter, the range of the force is clearly consistent with expectations for steric interactions for a slightly swollen chain. The force profile and images of $C_{12}E_3$ will be discussed separately below.

Figure 4 shows soft contact AFM images of the $C_{12}E_n$ adsorbed films on graphite ($n = 5$, 8, 9, 10, and 23). These images do not show the graphite surface, but rather the pattern of repulsive forces above it in solution. Images of $C_{12}E_{5-10}$ show an orderly pattern of stripes, whereas the image obtained for Brij 35 is of a featureless layer.

The stripes are quite straight and regular with periodicities of approximately 5.5 nm. This corresponds to the center-to-center spacing between hemicylindrical adsorbed micelles, as has previously been reported for ionic surfactants.[4,5,7] Also shown for comparison (Figure 4c inset) is a 2×2 nm filtered image of the graphite lattice underlying a $C_{12}E_9$ solution imaged in contact mode in the same orientation. The graphite lattice shows three symmetry directions. Note that the stripes in the adsorbed film are normal to one of the symmetry axes of graphite. This exemplifies the behavior of $C_{12}E_{5-10}$ self-assemblies on graphite and has also been observed previously.[4,5] Individual molecules are adsorbed aligned with a graphite symmetry axis, leading to self-assembly propagated in the orthogonal direction in the plane. The strong alignment by the substrate is also evident in Figure 4d, where two domains of adsorbed micelles meeting at a grain boundary are observed.

Unlike the other surfactants, the stripes of $C_{12}E_5$ (Figure 4a) are not straight but curve slightly. The surface also displays patches where no stripes are imaged. This is perhaps due to slight variations in applied force: higher force may appear to distort the stripes whereas lower force cannot resolve them. This may also be due to the proximity of the cloud point (Table 1), where steric stabilization forces are known to be highly sensitive to temperature.[25]

(27) Deguchi, K.; Meguro, K. *J. Colloid Interface Sci.* **1972**, *38*, 596.
(28) Drummond, C. J.; Warr, G. G.; Grieser, F.; Evans, D. F.; Ninham, B. W. *J. Phys. Chem.* **1985**, *89*, 2103.
(29) Rosen, M. J.; Cohen, A. W.; Dahanayake, M; Hua, X. *J. Phys. Chem.* **1982**, *86*, 541.
(30) Becher, P. In *Nonionic Surfactants*; Schick, M. J., Ed.; Marcel Dekker: New York, 1967.

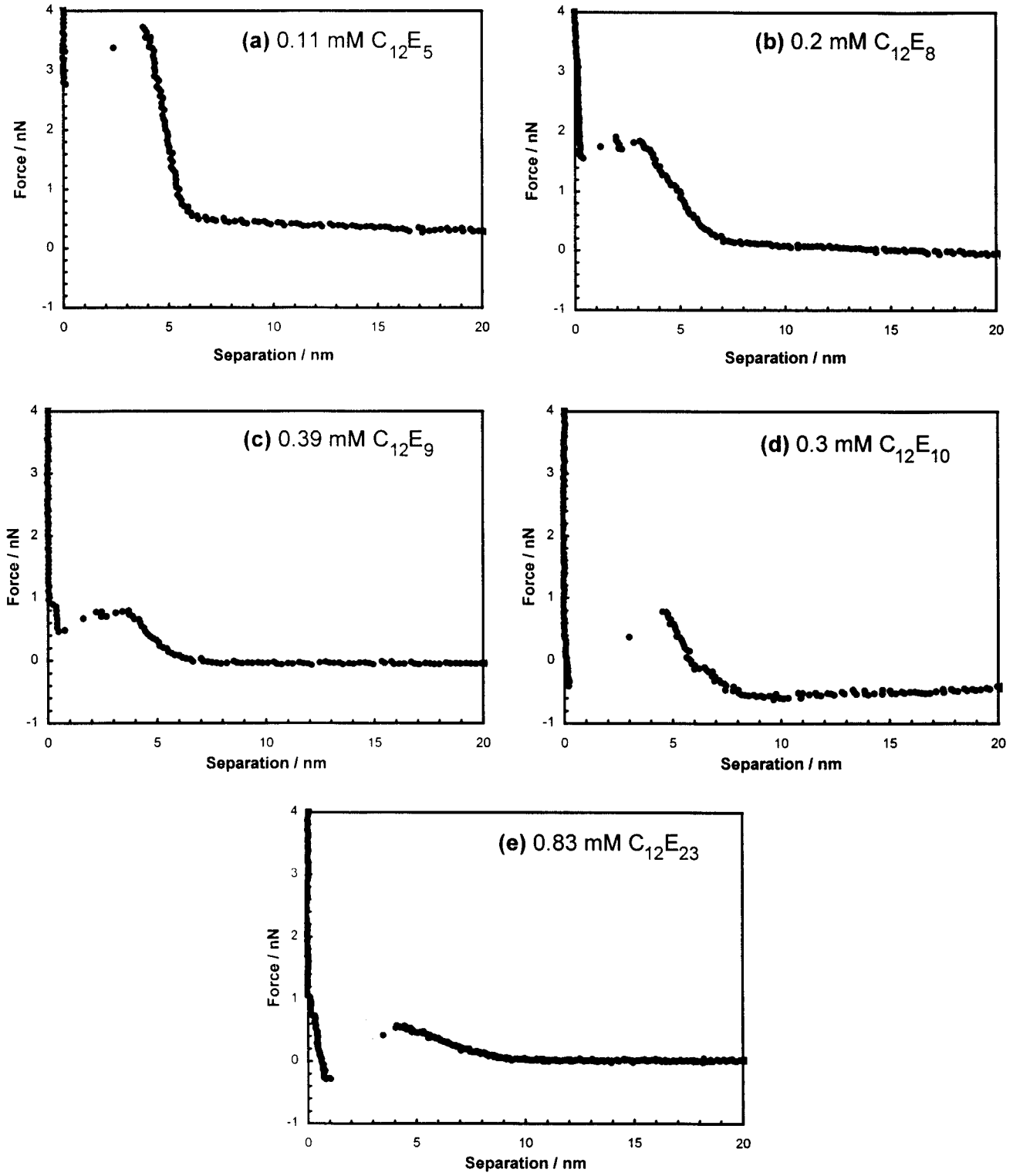

Figure 2. Force−distance profiles for nonionic surfactants on graphite: (a) 0.11 mM $C_{12}E_5$; (b) 0.20 mM $C_{12}E_8$; (c) 0.39 mM $C_{12}E_9$; (d) 0.30 mM $C_{12}E_{10}$; (e) 0.83 mM $C_{12}E_{23}$ (Brij 35).

Certainly adsorption isotherms are known to be sensitive to proximity to the cloud point.[13,31]

One might expect that the observed periodicities would also correlate with ethylene oxide chain length. Mitigating against this are several factors. First, the largest difference should be observed for $C_{12}E_5$ and $C_{12}E_{10}$, and the difference in radius of gyration of their head groups is small compared to the lateral resolution for soft contact imaging (see Figure 3). Second, we observe that the periodicity does depend to some extent on the scan orientation, as Wanless and Ducker[7] have discussed previously for SDS adsorbed on graphite. Finally, the extent to which the underlying graphite lattice determines, and possibly discretizes, this spacing is not known.

Figure 5 shows soft contact images of $C_{12}E_3$ on graphite at two concentrations: (a) 0.13 mM and (b) 0.75 mM. Force curves for $C_{12}E_3$ at the same concentrations are also shown in parts a and b of Figure 6. The lower concentration is below the solubility limit and is sufficient for a monolayer

(31) Ottewill, R. H. In *Nonionic Surfactants*; Schick, M. J., Ed.; Marcel Dekker: New York, 1967.

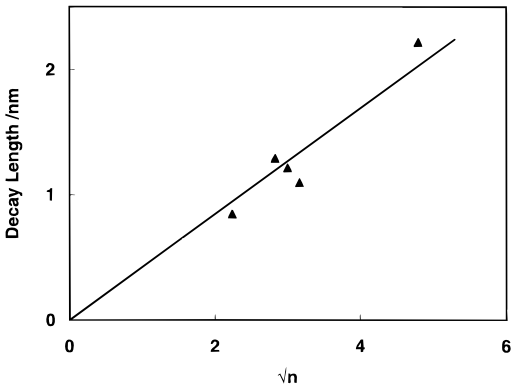

Figure 3. Decay length of the steric stabilization force for nonionic surfactants on graphite versus the square root of ethoxy chain length, n. Solid line indicates $n^{1/2}$ behavior expected for a random coil.

Table 2. Periodicities Observed in Adsorbed Films of Nonionic Surfactants on Graphite[a]

surfactant	periodicities/nm
$C_{12}E_3$	5.7, 34
$C_{12}E_5$	5.6 ± 0.2
$C_{12}E_8$	5.3 ± 0.3
$C_{12}E_9$	5.5 ± 0.2
$C_{12}E_{10}$	5.8 ± 0.5
$C_{12}E_{23}$	no structures

[a] These were determined from Fourier transform spectra of many different images with stripes in different orientations to the scan direction.

to form on the surface. The image is similar to $C_{12}E_5$ through $C_{12}E_{10}$, described above. However, here the force profile displays a strong attraction (Figure 6a) indicating that there is no steric barrier to contact. This all indicates a horizontal monolayer on the surface with individual surfactant molecules arranged tail-to-tail and head-to-head along one of the graphite symmetry axes, producing stripes normal to this which have a periodicity of 5.7 nm (Table 2).

The higher concentration solution appeared slightly cloudy but was transparent enough to allow images to be observed. At this concentration a second set of periodic stripes are observed, with a 34 nm repeat distance. Figure 5b shows the large period stripes with the 5.7 nm stripes visible between them. These appear to extend into solution further than the underlying stripes of the adsorbed film and were found to extend over wide regions of the surface, at least 3 μm.

The force curve also indicates that the higher concentration film extends into solution (Figure 6b) and exhibits multiple jumps on approach to the surface. This contrasts with the force profiles for the surfactants previously described where only one repulsive region and jump into contact is observed.

Discussion

The predominant image obtained from AFM studies of adsorbed ionic and zwitterionic surfactant films on graphite is one of periodic stripes.[4,5,7,8] These have been shown to be hemicylinders which form due to hydrophobic association of the alkyl tails over a horizontally adsorbed layer driven by the hydrophobic interaction between alkyl tails and graphite.

Stripes are also the main morphology observed in this work. In no system did we identify hemispherical or circular features, and in only one case was a featureless layer observed (thereby establishing that stripes are not an experimental artifact).

In order to interpret the observed film structures and the effect of the solid substrate on self-assembly behavior, we turn to the surfactant packing parameter. Recall that the packing parameter and the preferred self-assembly structure depend on both ethylene oxide number and volume fraction of amphiphile. These adsorbed films are surface saturated. The surface concentration is far greater than that in bulk solution so it is not appropriate to compare the interfacial self-assembly structure with the micellar phase, where surfactant micelles are present only in dilute solution. The comparison is more properly made with the first ordered lyotropic mesophase, where interaggregate interactions and surfactant concentrations are similar to those of a saturated surface.

This empirical correlation (see Table 1) would predict that $C_{12}E_8$ and $C_{12}E_{10}$, which both form a hexagonal phase, should produce aligned hemicylinders on graphite, just as we observe. $C_{12}E_9$ and $C_{12}E_{23}$ should both form hemispheres, and neither does. $C_{12}E_9$ instead forms stripes, hemicylinders like $C_{12}E_8$ and $C_{12}E_{10}$, and $C_{12}E_{23}$ forms a featureless layer. $C_{12}E_3$ and $C_{12}E_5$ are expected to form lamellae. This is not seen for $C_{12}E_5$ but is certainly consistent with the images obtained for $C_{12}E_3$ at high concentration. However if we are not too fussy about temperature, the existence of a bulk hexagonal phase for $C_{12}E_5$ a little below room temperature brings its aligned hemicylinder structure into the picture.

There are numerous remaining differences between expectations and observations in this scheme, but these all arise from one common source: the graphite substrate. The high degree of order and orientation of the stripes observed in these and other systems has been noted previously. Further to this, alkanes and aliphatic alcohols, which do not undergo self-assembly, also form similar striped structures on graphite.[32−34] The initial adsorption step for all amphiphilic molecules thus seems to be a templated adsorption of the aliphatic chain along one of the graphite symmetry axes up to coverage by a horizontal monolayer. The striped phase thus formed orients subsequent adsorption, which occurs through hydrophobic association. Support for this mechanism is provided by two-step adsorption isotherms of surfactants onto graphite.[12] Calorimetric studies also provide evidence for this behavior. Findenegg *et al.*[13] have described adsorption onto graphite as consisting of an initial "effectively irreversible" step, followed by a weaker, reversible adsorption, driven by hydrophobic aggregation of the surfactant.

The initial strong adsorption below the cmc is directly related to the adsorption of alkyl chains tail-to-tail along the crystal axes of graphite. Molecules adsorb along one of three symmetry axes of graphite, and further adsorption produces parallel stripes of molecules tail-to-tail and head-to-head perpendicular to these axes. These intimately adsorbed molecules form templates for further adsorption. This allows the development of hemicylindrical adsorbed micelles.

The initial film formed by $C_{12}E_3$ adsorbed on graphite at low concentration appears to be such a striped phase, with stripes oriented perpendicular to the underlying graphite lattice. That they are not hemicylinders is evidenced by the attractive jump into contact. At a higher concentration a more extended self-assembly structure develops over this initial layer, which we interpret as bilayers growing normal to the surface and templated by the striped phase.

(32) Groszek, A. J. *Proc. R. Soc. London, Ser. A* **1970**, *314*, 473−498.
(33) Yeo, Y. H.; Yackaboski, K.; McGonigal, G. C.; Thompson, D. J. *J. Vac. Sci. Technol.* **1992**, *A10*, 600−602.
(34) Rabe, J. P.; Buchholz, S. *Science* **1991**, *253*, 424−427.

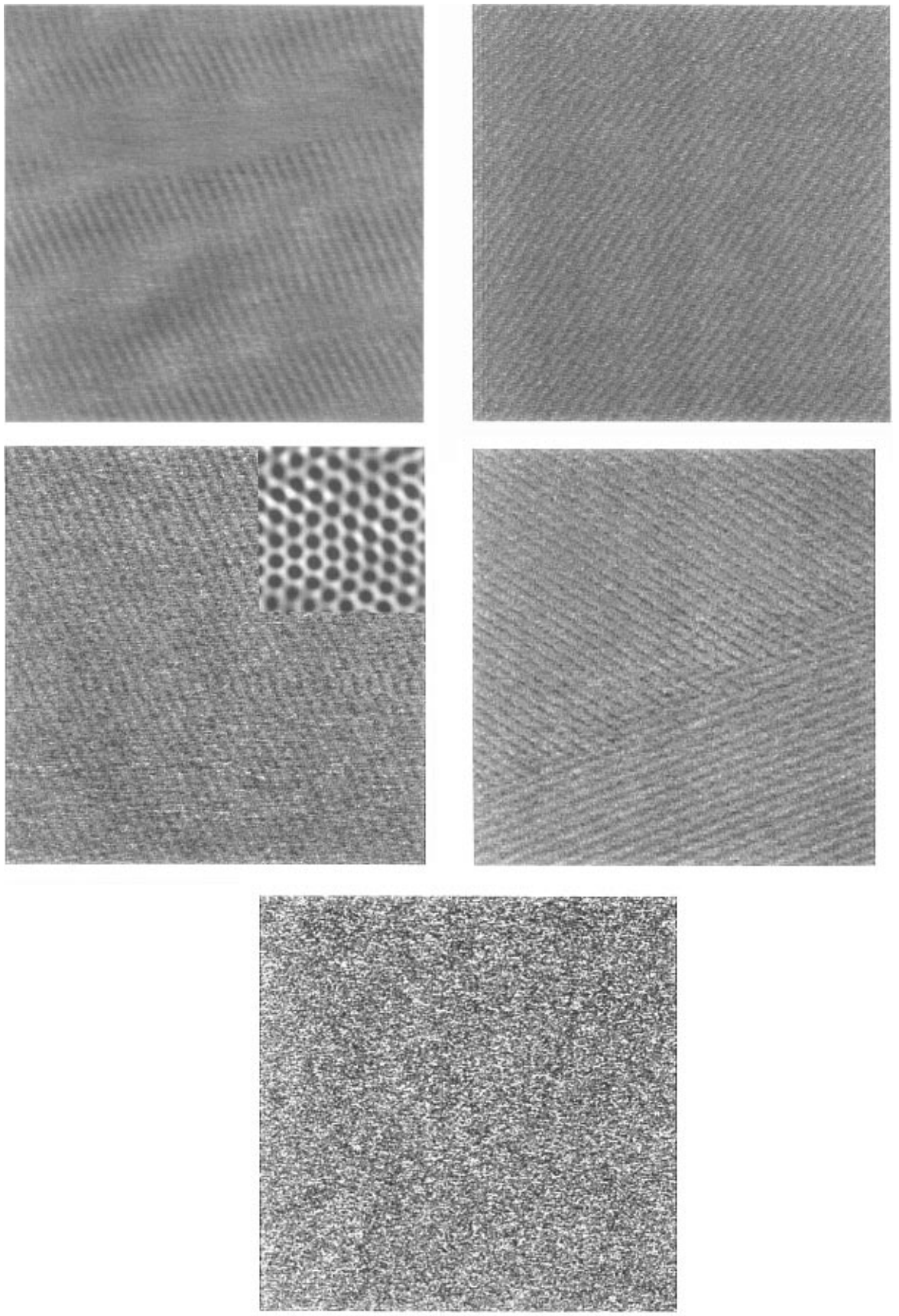

Figure 4. Soft contact images of nonionic surfactant adsorbed films on graphite: (a, top left) 0.11 mM $C_{12}E_5$; (b, top right) 0.2 mM $C_{12}E_8$; (c, middle left) 0.39 mM $C_{12}E_9$; (d, middle right) 0.3 mM $C_{12}E_{10}$; (e, bottom) 0.83 mM $C_{12}E_{23}$ (Brij 35). The image size is 200 × 200 nm in each case. Inset to (c) shows a contact mode 2 × 2 nm filtered image of the underlying graphite crystal lattice.

$C_{12}E_3$ forms only a lamellar mesophase in solution at all temperatures (Table 1), so hemicylinders seem to be precluded. In this case, preconcentration at any surface would predict bilayers. In addition the strong templating effect of graphite orients the alkyl tails of surfactant molecules tail-to-tail along the crystal axes. This arrangement forms the basis of a bilayer which can then propagate into solution. Thus $C_{12}E_3$, which forms lamellae

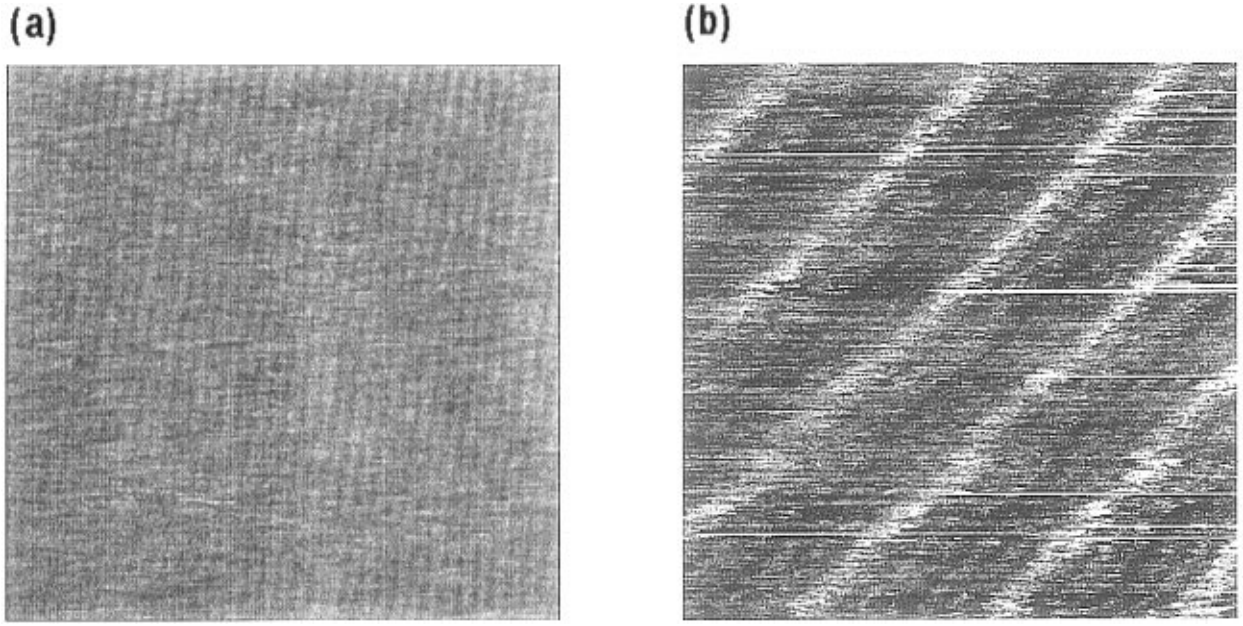

Figure 5. 200 × 200 nm AFM images of $C_{12}E_3$ on graphite at two concentrations: (a) 0.13 mM $C_{12}E_3$ which shows parallel stripes at repeat spacings of 5.7 nm; (b) 0.75 mM $C_{12}E_3$ showing regularly spaced major or higher bilayers of surfactant at repeat spacings of 34 nm with the lower bilayers of repeat spacings 5.7 nm seen in (a) between them. The major periodicity of 34 nm exists over wide regions of the graphite surface.

in solution, forms a lamellar phase at the graphite–solution interface normal to the surface.[35]

The force–distance curve at this concentration (Figure 6b) shows multiple maxima separated by jumps, unlike the other surfactants studied. While the curve shown is typical, the number of peaks in the force curve was not reproducible. At least three peaks (and often more) were always observed, and overall a peak-to-peak spacing of 2.5 nm was evident. The observed force curves are highly reminiscent of studies of confined lamellae using the surface force apparatus.[36,37] There the jumps correspond to "squeezing out" of free lamellae between the surfaces as they approach. In the AFM a similar mechanism may apply, leading to the observed sequence of repulsions followed by jumps as the tip ruptures or squeezes aside successive lamellae as it approaches the surface.

The complex force curve observed here suggests that the scanning capabilities of the AFM may be able to be used to develop a picture of the near-surface structure of complex fluids above the adsorbed layer, and this is currently being investigated.

We conclude from the force curve that there are lamellae present in the space between the graphite surface and the probe tip at large separations, and that these are oriented in the usual direction, that is, parallel to the solid substrate. This is further supported by the fact that no lateral structure can be imaged at low force (large distances). When the tip is brought near to contact, however, the images shown in Figure 5 are obtained, which we interpret to be vertical bilayers anchored to the underlying stripe phase.

These bilayers are regularly spaced; however the observed repeat spacing of 34 nm is not that which occurs in $C_{12}E_3$ bulk lamellar phase. (The bulk phase spacing for this sample is 4 nm.) The repeat spacing observed on the substrate corresponds to six of the underlying "stripes," suggesting again that the graphite lattice plays an important role in modulating interfacial self-assembly. This registry between anchored bilayers and its relationship to equilibrium spacing in bulk is currently the subject of further investigation. For the present we are concerned only with the geometry of the interfacial structure.

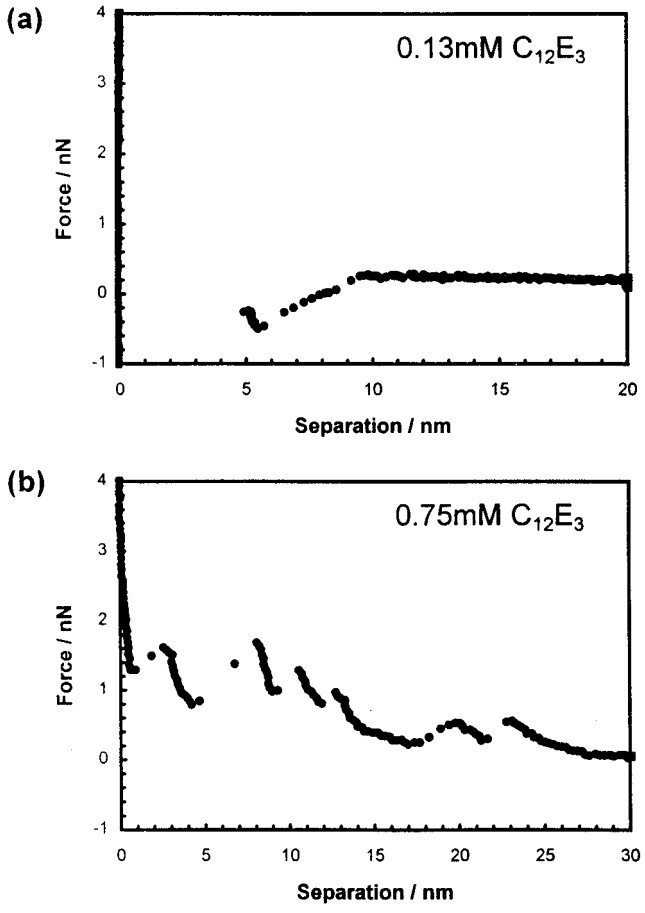

Figure 6. Force–distance curves for $C_{12}E_3$ at (a) 0.13 mM and (b) 0.75 mM.

(35) Solutions of SDS on graphite have also been reported to exhibit long-range periodic structures with large spacings after long adsorption times.[7] SDS and the cosurfactant dodecanol, its hydrolysis product, certainly form a lamellar phase in solution. This suggests that a lamellar phase anchored to the surface was imaged in this case.

(36) Kekicheff, P.; Richetti, P.; Christenson, H. K. *Langmuir* **1991**, *7*, 1874.

(37) Richetti, P.; Kekicheff, P.; Barois, P. *J. Phys. II* **1995**, *5*, 1129.

The graphite substrate also influences things at the other extreme of packing geometry. The initial strong adsorption along the graphite symmetry axes ensures that hemispherical adsorbed micelles are not able to form. To achieve this, strongly bound molecules would need to rearrange into a circular base from parallel stripes. For $C_{12}E_9$, which displays a bulk hexagonal phase at higher concentration than its cubic phase, hemicylinders remain the equilibrium structure and an adequate solution to the problem of minimizing free energy under the constraint of strongly adsorbing alkyl chains.

The large head group of $C_{12}E_{23}$ produces a molecular geometry which is unable to form less curved structures than spheres at any composition in bulk solution (Figure 1). That the alkyl tail is strongly adsorbed onto graphite is clearly established from the force profile (Figure 2). We assume that the alkyl chain is horizontally adsorbed as for the other homologues, although we have no way of imaging this directly. The large head group of 23 ethylene oxide units sterically prohibits a hemicylindrical micelle and probably severely limits the extent to which alkyl chains may align into stripes. In this extreme case an adsorbed layer is formed which is featureless under the AFM. We infer that this is composed of individually anchored molecules each sheltered from water by their large, hydrated hydrophilic chain (head groups). Just as in the bulk, the large head group dominates the surface structure; however the graphite induces a very different equilibrium structure.

The observed interfacial self-assembly structures can be rationalized in terms of packing considerations, just as in bulk; however a different set of constraints apply. In bulk self-assembly, geometry is determined by a radius of curvature that is identified with the length of the alkyl chain of the surfactant. At a graphite surface which has particularly strong anisotropic interactions with the alkyl chains, the more rigorous constraint is a radius of curvature normal to the surface plus a preferred orientation direction. Even an amorphous hydrophobic surface should be less proscriptive, perhaps allowing hemispheres, and at other surfaces different constraints will obtain.

Except under extreme or unusual conditions, we therefore see why surfactants tend to aggregate into aligned, hemicylindrical structures on graphite. To pursue the analogy with bulk self-assembly, this is akin to the observation that most micelles are spheres near the cmc, even if they soon transform to rods with increasing concentration or if they never form an I_1 cubic phase. Smaller aggregation numbers increase the configurational entropy of the system. Perhaps the same principle is at work at the interface. Given that spheres are precluded, even surfactants which might form lamellae at high concentrations initially form hemicylinders because the entropy debt incurred by removing surfactants from dilute solution to organize them in an anchored bilayer is not repaid by the energy gained by hydrophobic association. The cost of a slightly changed interfacial curvature is evidently preferred for $C_{12}E_5$, but not for $C_{12}E_3$. Our results indicate that if a cylindrical self-assembly geometry exists anywhere in the bulk phase diagram, then hemicylinders will form on graphite. Other morphologies only arise when this state is precluded.

Conclusions

Thus $C_{12}E_3$, geometrically capable of only forming bilayers as a bulk lyotropic phase, forms them perpendicular to the graphite surface. $C_{12}E_5$, $C_{12}E_8$, and $C_{12}E_{10}$ form cylindrical micelles in solution and hemicylinders at the surface. $C_{12}E_9$ forms a cubic phase of spherical micelles in bulk, but strong interactions with graphite induce hemicylinders at the surface. $C_{12}E_{23}$ cannot accommodate a hemicylinder and instead forms a laterally unstructured layer with large head groups protruding into solution. When applied with due consideration of the effect of the substrate interaction, the surfactant packing parameter provides a useful framework for interpreting adsorbed layer structure, just as it does for bulk self-assembly.

Acknowledgment. This work was funded by the Australian Research Council and the US Army Research Office (Grant DAAH04-95-1-0102) and was made possible by the University of Sydney Special Studies Program. H.N.P. acknowledges the receipt of an Australian Postgraduate Award and a Jim O'Donnell postgraduate travel grant from the Royal Australian Chemical Institute. We thank Digital Instruments for technical support.

LA9702547